UCLA

Title

Identification, Model Updating, and Response Prediction of an Instrumented 15-Story Steel-Frame Building

Permalink

Authors

Skolnik, Derek
Lei, Ying
Yu, Eunjong
et al.

Publication Date

2006-05-05

Peer reviewed

Identification, Model Updating, and Response Prediction of an Instrumented 15-Story Steel-Frame Building

Derek Skolnik,[a)]Ying Lei,[b)]Eunjong Yu,[b)]and John W. Wallace,[c)]M.EERI

Identification of the modal properties of the UCLA Factor Building, a 15-story steel moment-resisting frame, is performed using low-amplitude earthquake and ambient vibration data. The numerical algorithm for subspace state-space system identification is employed to identify the structural frequencies, damping ratios, and mode shapes corresponding to the first nine modes. The frequencies and mode shapes identified based on the data recorded during the 2004 Parkfield earthquake ($M_w = 6.0$) are used to update a three-dimensional finite element model of the building to improve correlation between analytical and identified modal properties and responses. A linear dynamic analysis of the updated model excited by the 1994 Northridge earthquake is performed to assess the likelihood of structural damage. [DOI: 10.1193/1.2219487]

INTRODUCTION

The UCLA Factor Building was instrumented by the U.S. Geological Survey with an embedded 72-channel accelerometer network following the 1994 Northridge earthquake. The accelerometer network is distributed throughout the building and is continuously recording building vibrations. In December 2003, the sensor network was upgraded by installing state-of-the-art data-logging equipment and fiber-optic network cables. To date, substantial data have been collected from ambient vibrations under different environmental conditions, as well as from low-amplitude vibrations from several earthquakes, including the Parkfield earthquake of 28 September 2004. The Factor Building, with its embedded sensor network, provides a unique platform for the identification of dynamic characteristics, structural performance monitoring, and damage detection. Establishing a reliable three-dimensional finite-element (FE) model that accurately represents the mass and stiffness of the structural system is an important step in assessing the structural performance and detecting damage under significant shaking.

Of the many existing system identification algorithms, the advanced numerical algorithm for subspace state-space system identification (N4SID) (Van Overschee 1994) is utilized in this paper. N4SID allows numerically reliable state-space models to be ob-

[a)]Graduate Student, Department of Civil & Environmental Engineering, University of California, Los Angeles, CA 90095

[b)]Postdoctoral scholar, Department of Civil & Environmental Engineering, University of California, Los Angeles, CA 90095

[c)]Professor, Department of Civil & Environmental Engineering, University of California, Los Angeles, CA 90095

tained for complex multivariable dynamic systems directly from measured data. Structural system identification can be accomplished using both the measured input and output data, or just measured output data. The N4SID approach is particularly useful when the number of outputs and the number of states (the order of the system) are relatively large. The identification of frequencies, mode shapes, and damping ratios for the Factor Building is accomplished using vibration measurements obtained during the Parkfield earthquake as well as under ambient vibrations.

An initial FE model is created based on architectural and structural drawings. The model is updated using identified modal properties from the Parkfield earthquake in order to achieve modal properties and response that closely match those measured. There are two well-established strategies for FE model updating (Friswell 1995). One method updates the system stiffness and mass matrices directly, whereas the other updates physical properties of the FE model (e.g., material- and geometry-based properties). The parameters in each method are updated by an iterative solution of an optimization problem that minimizes the error between the model and identified properties. In the latter method, there is physical significance associated with the updating of the model parameters, which is advantageous. Parameters to be updated can be selected to represent properties of the building that are not readily modeled, such as stiffness contribution of nonstructural components (NSCs) and the mass provided beyond the self-weight of the structure; therefore, this approach is adopted.

Details of the identification, FE modeling, and updating processes are described in the following sections. A linear dynamic analysis of the updated model excited by the 1994 Northridge earthquake is performed using the provisions set forth in *FEMA-356* (ASCE 2000) to assess whether structural damage was likely to have occurred for this event.

BUILDING DESCRIPTION AND INSTRUMENTATION

The UCLA Doris and Louis Factor Health Science Building (Figure 1) is home to several centers for the heath sciences, including the School of Nursing, the Jonsson Comprehensive Cancer Center, as well as other biomedical facilities. Designed and constructed in the late 1970s, the 15-story, 216.5-foot-high building is the tallest on campus. The structural system consists of a Type-I (three-hour fire rating per the 1973 *Uniform Building Code* [ICBO 1973]) steel special moment-resisting frame (SMF) supported by concrete bell caissons and spread footings. There are two basement levels. The floor area for floors 10-16 (roof) increases by approximately 13.5% due to a slight overhang on the east and west faces of the building, as shown in Figure 2.

A typical floor plan, shown in Figure 2, displays the orientation of the seismic framing system. For the most part, the building is symmetric about the east-west axis (adopted as the x direction in the analytical model, where east is positive) and slightly asymmetric about the north-south axis (adopted as the y direction where north is positive). Each floor consists of a $6\frac{1}{4}''$ thick lightweight concrete slab on $3''$ metal decking and a Norman face brick veneer anchored to the floor. A glass curtain wall consists of $1/4''$ spandrel glass supported with an aluminum frame. The 15th story houses mechani-
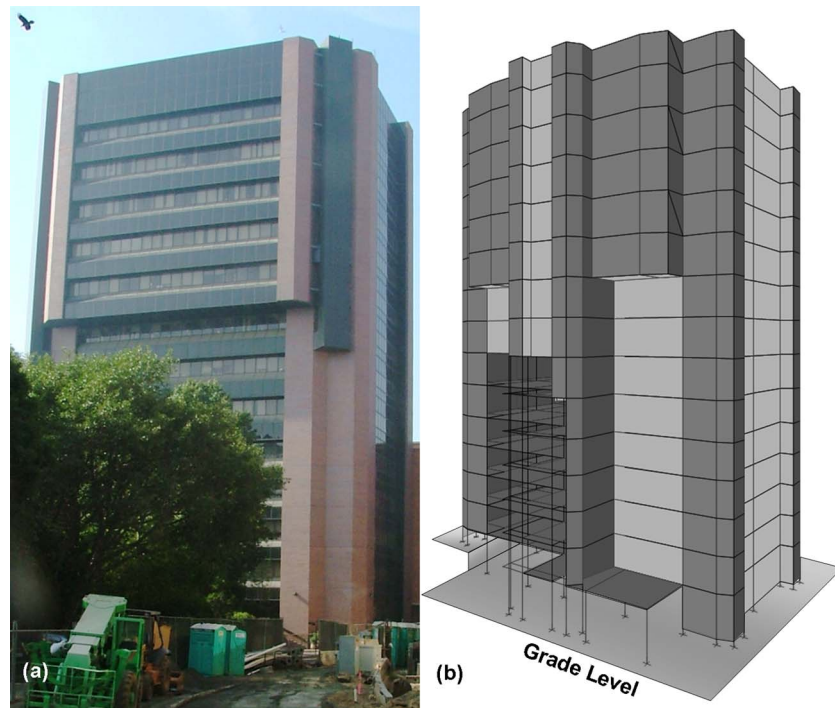
Figure 1. (a) Louis Factor Building showing east face, and (b) finite element model of the building showing west face.

cal equipment. Additional details are available in the first author's master's thesis (Skolnik 2005).

During the 1994 Northridge earthquake, the Factor Building suffered damage to the exterior brick veneer. A post-earthquake damage evaluation was performed (Englekirk 1994). Several SMF joints at the 13th and 14th floors were selected for visual and ultra-sonic inspection because they corresponded to areas where the brick veneer appeared to have bulges when viewed from the roof. No cracks in the welds were found at these joints and the nonstructural damaged was quickly repaired.

Following the 1994 Northridge earthquake, the U.S. Geological Survey instrumented the structure with 72 uniaxial force-balanced accelerometers with an on-site recording system. Four accelerometers are installed at each floor above grade, oriented to record translational motions near the perimeter of the floor (two in each direction), as shown in Figure 2 and Table 1. Each of the two basement levels has an accelerometer to record each translational direction, as well as two accelerometers to record vertical responses.

In December 2003, the building sensor network was upgraded using funds provided primarily by the NSF Science and Technology Center for Embedded Networked Sensing (CENS) headquartered at UCLA. The upgrade consisted of converting all 72 channels to
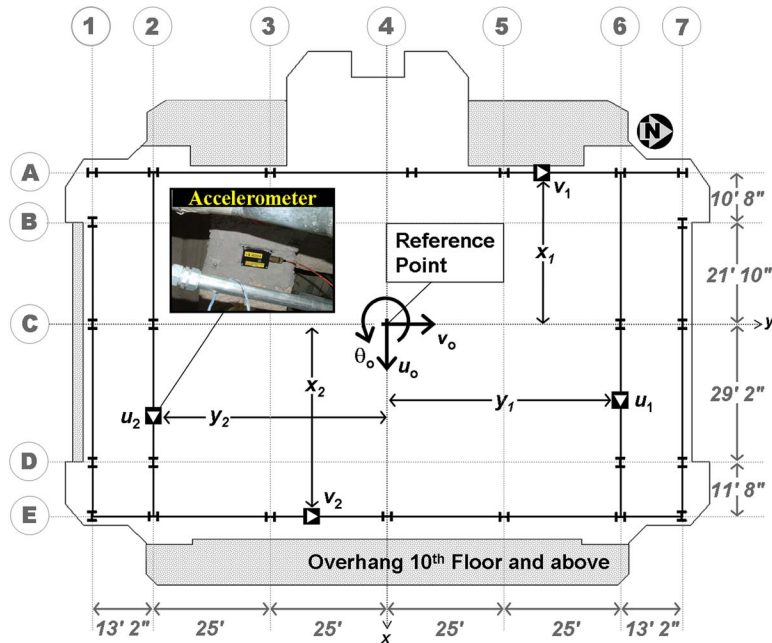
Figure 2. Typical Factor Building floor plan, sensor locations, derived story accelerations (u_o, v_o, and θ_o) and the selected point of reference, and positive directions.

a 24-bit network continuously recording data viewable via the Internet in real time. This reconfiguration included the installation of nine, eight-channel Q4120 A/D data loggers recording at 100 and 500 samples per second, resulting in approximately 3 gigabytes/day of data that are stored on a 1.5-Terabyte RAID array. In February 2005, a 330-foot-deep borehole seismometer was installed approximately 160 feet away from the building. The level of instrumentation provided in and around the Factor Building makes it one of the most (if not the most) densely permanently instrumented buildings in North America.

VIBRATION DATA

The sensor network is continuously recording data and has recorded several small earthquakes, including the Parkfield, California, earthquake ($M_w = 6.0$) on 28 September 2004 at 10:15 a.m. PDT. According to the USGS Earthquake Hazards Program (2004), the earthquake epicenter was located approximately 163 miles from the Factor Building and peak acceleration of only 0.0025 g were recorded at the roof of the building. In addition, data collected on 29 April 2004 (Thursday) at 3:00 a.m. are extracted to establish an ambient vibration data set. This date and time are selected as to minimize the effects of traffic inside and outside of the building. The collected raw data are detrended to remove any signal bias and/or linear trends. Decimating the data at a lower sample rate

Table 1. Sensor coordinates with respect to selected reference point

Floor	Height (ft)	u_1 x (in)	u_1 y (in)	u_2 x (in)	u_2 y (in)	v_1 x (in)	v_1 y (in)	v_2 x (in)	v_2 y (in)
Roof	216.5	−354	300	490	−600	−390	300	490	−600
15th	205	−390	300	490	−600	−390	300	490	−600
14th	190	−96	600	175	−600	−390	−36	490	−48
13th	175	32	600	290	−600	−390	0	490	−48
12th	160	290	600	132	−600	−390	−12	490	−252
11th	145	170	600	−48	−600	−390	−70	490	−192
10th	130	60	600	182	−600	−390	450	490	−84
9th	115	84	600	204	−600	−390	15	350	−150
8th	100	218	600	−120	−600	−390	216	350	−120
7th	85.0	−166	600	120	−600	−390	219	350	−214
6th	70.0	88	600	36	−600	−390	210	350	−48
5th	56.5	120	600	36	−600	−390	228	350	−12
4th	43.0	100	600	50	−600	−390	−40	350	−250
3rd	29.5	170	600	75	−600	−390	45	350	−225
2nd	16.0	156	600	175	−600	−390	123	350	−150
1st	0.0	394	600	−25	−758	−390	−360	490	−240
A	−14.5	−48	−600	−132*	−300*	NA	NA	NA	NA
B	−28.0	−647	132	−390*	−600*	350	0	−490*	−600*

* Location of sensors recording vertical responses

removes high-frequency noise and reduces the data size. Data processing is performed using built-in functions (i.e., detrend, resample) of the MATLAB Signal Processing Toolbox. (MATLAB 2004)

For each floor above ground, the processed data collected from the four uniaxial accelerometers (u_1, u_2, v_1, and v_2) are used to compute the story accelerations (u_0, v_0, and θ_0) at the selected reference point in Figure 2 with the following equations:

$$u_1 = u_0 - y_1\theta_0 \quad u_2 = u_0 - y_2\theta_0 \quad v_1 = v_0 - x_1\theta_0 \quad v_2 = v_0 - x_2\theta_0 \tag{1}$$

where x and y are the respective coordinates of the corresponding accelerometer relative to the reference point, Table 1. Note that there are more equations than unknowns; therefore, the system of equations is overdetermined and a least-squares solution is used. Sixty-four of the 72 sensors were used (the unused 8 are installed in the basement floors) to derive the orthogonal components of the building's motion. Figure 3 displays the east-west (u_0) acceleration history during the Parkfield earthquake for selected floors. Figure 4 displays the smoothed Fast Fourier transforms (FFT) of Factor's story accelerations in response to Parkfield and ambient vibrations.
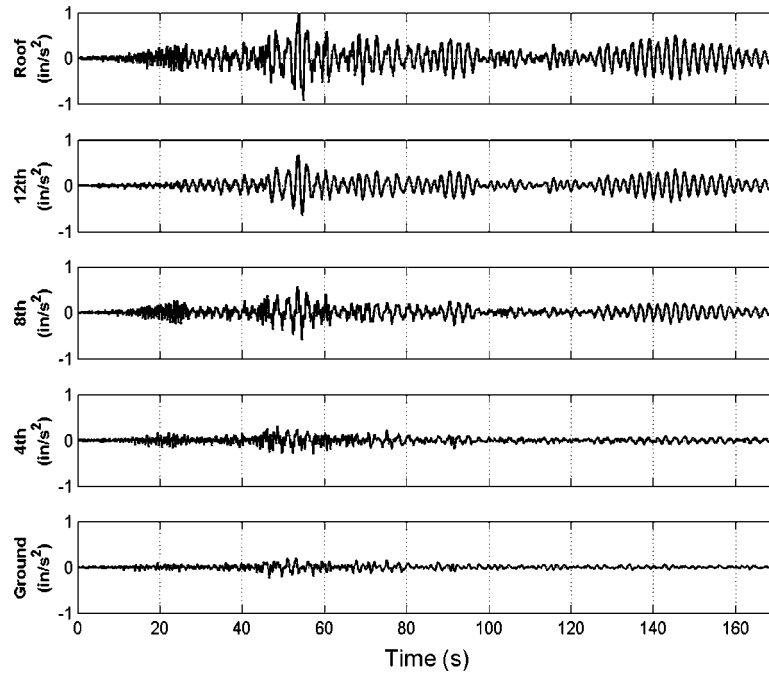
Figure 3. East-west story accelerations from sensor recordings during 2004 Parkfield, California, earthquake, for select floors.

IDENTIFICATION OF MODAL PROPERTIES

Of the many existing system identification algorithms, one advanced method available is the numerical algorithm for subspace state-space system identification (N4SID) (Van Overschee 1994). This approach offers numerically reliable state-space models for complex multivariable dynamical systems directly from measured data. No nonlinear search or iteration is performed, thus the computational complexity is modest compared with other system identification algorithms. In addition, the N4SID algorithm has been implemented in the System Identification Toolbox of MATLAB (2004).

It is well known that a linear time-invariant structural model can be described by the discrete first order differential equation in the state-space at the kth time step as

$$X_{k+1} = AX_k + BU_k$$

$$Y_k = CX_k + DU_k$$

(2)

where X is the state vector, A is the state matrix, B is the input influence coefficient matrix, C is the real output influence matrix, D is the output control influence coefficient matrix, U is the observed input, and Y is the output vector. In practice, there are always
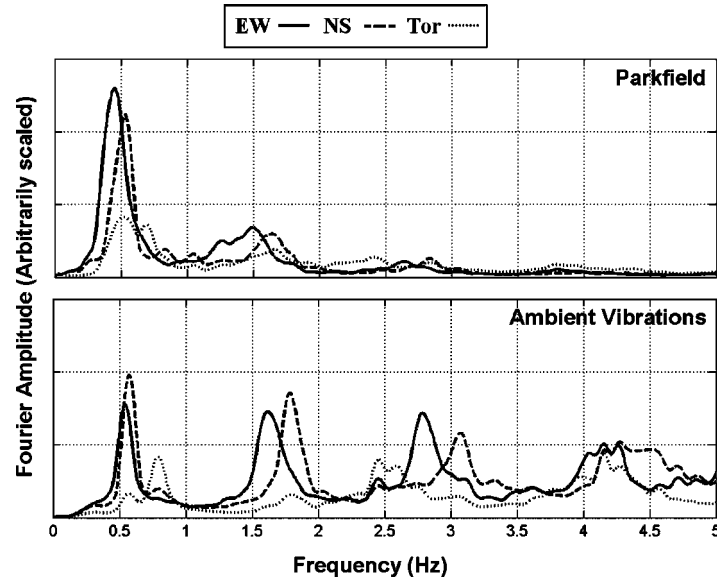
Figure 4. Arbitrarily scaled smoothed fast Fourier transforms of the EW, NS, and torsional floor accelerations for both Parkfield earthquake and ambient vibrations. Note that the two plots have different scaling.

system uncertainties such as measurement noise (ν) and process noise (ω); therefore, Equation 2 can be extended as

$$X_{k+1} = AX_k + BU_k + \omega_k$$
$$Y_k = CX_k + DU_k + \nu_k \tag{3}$$

It is assumed that the ω and ν are uncorrelated zero-mean stationary white noise vector sequences (Ljung 1999). In the case of ambient noise, it is impossible to measure the input term U; therefore, it is modeled as white noise using the term ω as

$$X_{k+1} = AX_k + \omega_k$$
$$Y_k = CX_k + \nu_k \tag{4}$$

The white noise assumption for ambient noise can be omitted; however, if the input contains some dominant frequency components in addition to white noise, then those frequency components cannot be separated from the eigenfrequencies of the system and they will appear as poles of the state matrix A.

Subspace state-space system identification algorithms mainly consist of two steps. The first step involves making projections of certain subspaces generated from the input/output observations to estimate the state vector (X_k) of the system. This is done using

linear algebra tools such as QR decomposition and singular value decomposition (SVD) (Ljung 1999). The second step retrieves the system matrices A, B, C, and D from the estimated states based on a linear least-squares solution.

After the mathematical description of the structure (the state-space model) is found, it is then straightforward to determine the modal parameters: natural frequencies (f), damping ratios (ζ), and mode shapes (ϕ). The complex eigenvalues (λ) and eigenvectors (ψ) of the damped system can be calculated from the system matrix A. If the damping is assumed to be small and nearly classical, then the modal properties of the undamped structure can be approximated as (Safak 1991, Alvin 1994)

$$f_i = |\lambda_i|/2\pi \quad \zeta_i = \mathrm{Re}(\lambda_i)/2\pi f_i \quad \phi_i = |C\psi_i| \cdot \mathrm{sign}[\mathrm{Re}(C\psi_i)] \tag{5}$$

for the ith mode where $\mathrm{Re}(\bullet)$ and $\mathrm{sign}[\bullet]$ denote the real part and the algebraic sign of $\bullet$.

For data corresponding to the Parkfield earthquake, sensors on the ground floor measure the input; therefore, the excitation is known. For the ambient vibration data, the excitation is not measured (is unknown) and the system takes on the form of Equation 4.

Implementation of the N4SID algorithm requires determining the order of the state-space model (dimension of state vector; X_k), which is a challenging problem. Theoretically, the order of the state-space model can be determined from the number of the non-zero singular values in the SVD process. In general, an N-degree-of-freedom (DOF) system will have a state-space model order of 2N. Assuming rigid diaphragms and ignoring vertical DOFs, the Factor Building has three degrees of freedom for each of the 15 floors, resulting in a 45-DOF system. However, due to measurement noise and the non-white-noise nature of unknown excitation (in the case of ambient vibration), a model order higher than 90 is needed in order to extract as many modal parameters as possible. As a consequence of high model orders, the algorithm identifies "superfluous" or "nonstructural" modes.

To distinguish the structural modes from the superfluous modes, stability plots are employed (Bodeux 2001). As the model order increases, the identified structural modes (and hence associative modal properties) should remain reasonably stable. Stability tolerances are chosen based on the change in frequency (Δf), change in damping ratios ($\Delta \zeta$), and modal assurance criterion (MAC) (Link 1999). In this paper, stable modes for a given model order are defined as modes where all three of the following convergence criteria are met:

$$\Delta f < 1\% \quad \Delta \zeta < 5\% \quad MAC > 99\% \tag{6}$$

Figure 5 displays the stability plot for model identification using data from the Parkfield earthquake. The final modal properties are selected as the stable modes of the highest model order and are displayed in Table 2 and Figure 6.

From inspection of Table 2, a stiffer structure with substantially reduced higher-modal damping ratios is identified by use of ambient vibration data relative to use of the
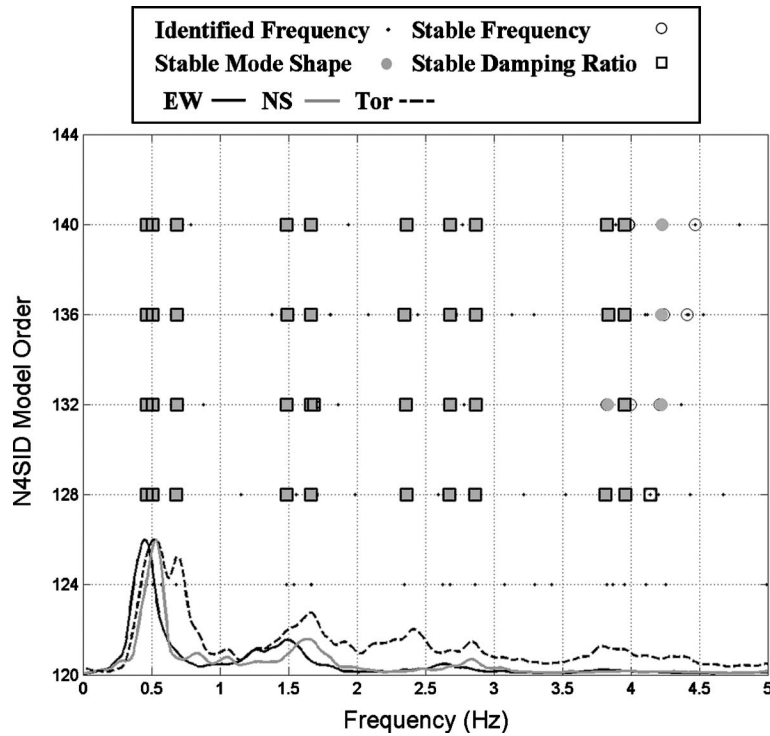
Figure 5. Stability plot with FFTs for system identification results using recorded responses to the Parkfield earthquake. The *y*-axis represents the increasing user-selected model order.

earthquake data. This phenomenon is generally believed to be the result of nonstructural components (NSCs) contributing more stiffness (Kohler 2005) and a broader excitation bandwidth at low amplitude than at higher-amplitude vibrations.

Table 2. Identified modal properties

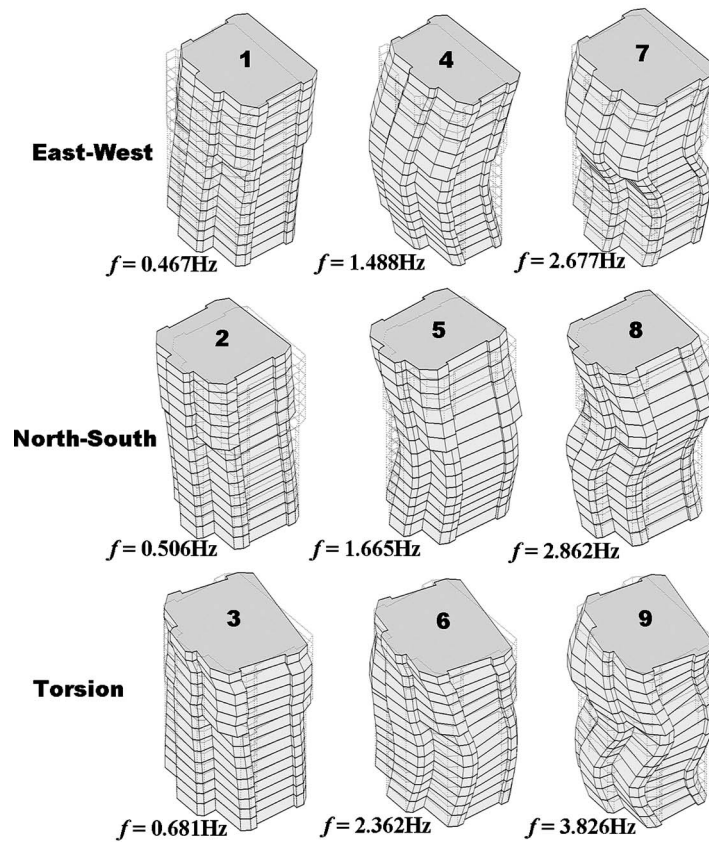| Mode Shape		Ambient Vibrations		Parkfield EQ		Difference	
No.	Direction	Freq (Hz)	Damp (%)	Freq (Hz)	Damp (%)	Freq (%)	Damp (%)
1	EW	0.545	5.1	0.467	4.8	14.3	5.9
2	NS	0.588	8.3	0.506	4.7	13.9	43.4
3	Torsion	0.807	10.8	0.681	5.8	15.6	46.3
4	EW	1.626	2.1	1.488	5.4	8.5	−157.1
5	NS	1.795	1.4	1.665	4.9	7.2	−250.0
6	Torsion	2.485	2.9	2.362	7.4	4.9	−155.2
7	EW	2.825	2.2	2.677	4.4	5.2	−100.0
8	NS	3.061	1.3	2.862	4.9	6.5	−276.9
9	Torsion	4.017	2.9	3.826	4.6	4.8	−58.6

Figure 6. First nine identified mode shapes and frequencies using Parkfield earthquake data.

The Factor Building's dense sensor array allows for recordings at each DOF (of the assumed model); therefore, the identified mode shapes are complete. For a data set with missing records at some DOFs, the mode shape elements associated with the missing DOF cannot be identified and linear interpolation is needed to fill in the gaps.

FINITE ELEMENT MODELING

An initial FE model of the Factor Building is established based on architectural and structural drawings (see Figure 1). Traditionally, a model of only the lateral-force resisting system is used for design of buildings subjected to strong ground motions. However, when considering the dynamic behavior of a building under ambient and/or small-amplitude vibrations, the gravity frame, as well as other NSCs (e.g., brick veneer and interior partitions), may substantially contribute to the lateral stiffness. For this reason, the gravity columns and girders are included in the FE model, while the NSCs, which are not as readily modeled, are addressed later.
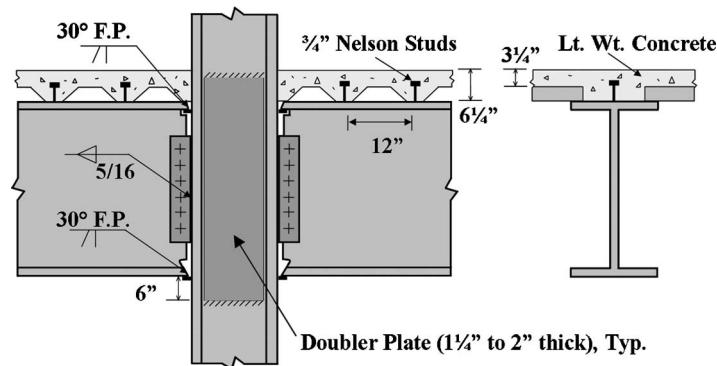
Figure 7. Typical moment-resisting connection details for a girder to column flange.

For structures with SMFs, proper modeling of connection behavior is critical (Bruneau 1998). Figure 7 shows Factor's typical fully restrained moment connection for a girder-to-column flange connection, which consists of full penetration welds, doubler plates, and bolted shear tabs. Partially restrained connections, typically within the gravity frame, include web shear tabs; however, the girder and column flanges are not welded. Since the FE model of the Factor Building is presently used to predict responses at low-level vibrations, it is assumed that the partially restrained connections act as fully restrained.

Another important modeling issue for steel moment frames involves assessing the rigidity of the panel zones. Generally, FE programs allow users to assign rigid-end offsets, calculated according to joint geometry, and a rigidity factor corresponding to the effective length of the rigid-end offset. Although rigid-end offsets are purely geometrical attributes, the rigidity factor can be adjusted to better represent the rigidity/flexibility of joints. Based on general practice, a recommended average value of 0.5 for the rigidity factor is applied (Leger 1991).

It is common design practice to employ composite action between the reinforced concrete floor slab and the steel girders by embedding shear studs, welded to the top flange of floor beams, into the concrete deck. The extent of the composite action depends on the number and spacing of shear studs (Figure 7). Rather than modeling the concrete slab with cumbersome shell elements, it is common to model the composite section with an effective moment of inertia. For low-amplitude vibrations, it is assumed that no slip occurs between the steel flange and bottom of the metal decking, allowing for straightforward calculation of the composite moment inertia. FE software typically allows for modification factors to be applied to the geometric properties of the model components. The moment of inertia of the moment frame girders (W-sections) are multiplied by the modification factors (ranging from 1.5 to 2.5) to model the properties of the composite sections.

Table 3. Estimated mass quantities from architectural drawings

| | Floor System | | Exterior Wall System | |
Conc. Deck	Partitions	Mech. Equip.	Brick Veneer	Curtain Wall
46 psf	10 psf	5 psf	25 psf	5 psf

The foundation is modeled as a fixed base. Due to the change in elevation (see Figure 1) the base is set at the 1st floor on the south side and the 2nd floor on the north side. This common assumption simplifies the modeling procedure but ignores the potentially important effect of soil structure interaction. However, during low-amplitude vibrations such as the Parkfield earthquake, these effects are most likely negligible, particularly for a flexible SMF building (Stewart 1999).

In order to accurately represent the building mass distribution, shell elements of prescribed densities and negligible stiffness are added to the FE model.

Table 3 includes a list of estimated mass quantities that were used for the floor and exterior wall systems. As with the NSCs, the live load and the superimposed dead load (i.e., fixed equipment not part of structures self-weight) are neglected and the potential contribution of these parameters is addressed in a subsequent section.

Under the assumption that floor diaphragms are rigid in plane and masses are lumped at the center of mass at each floor level, mass (M) and stiffness (K) matrices are extracted from the FE model. The modal properties of the undamped system are obtained by solving the eigenvalue problem. Frequencies and mode shapes for the first nine modes of this initial analytical model are compared to those identified using the Parkfield earthquake data in Table 4. Not only is there considerable discrepancy between identified and analytical frequencies, the order of NS and EW modes is reversed.

Table 4. Modal property comparison between identified and analytical models

| Mode Shape		Identified from Parkfield	Initial Model			Updated Model		
No.	Dir.		Freq (Hz)	Error (%)	MAC (%)	Freq (Hz)	Error (%)	MAC (%)
1	EW	0.467	0.513	−9.9	99.9	0.473	−1.3	99.8
2	NS	0.506	0.511	−1.0	99.6	0.514	−1.6	99.9
3	Torsion	0.681	0.666	2.2	99.9	0.691	−1.5	99.2
4	EW	1.488	1.507	−1.3	99.7	1.507	−1.3	99.2
5	NS	1.665	1.445	13.2	98.1	1.670	−0.3	98.5
6	Torsion	2.362	1.903	19.5	97.8	2.319	1.8	98.3
7	EW	2.677	2.534	5.3	98.9	2.580	3.6	99.3
8	NS	2.862	2.386	16.6	94.5	2.761	3.5	98.9
9	Torsion	3.826	3.185	16.7	94.3	3.743	2.2	99.2
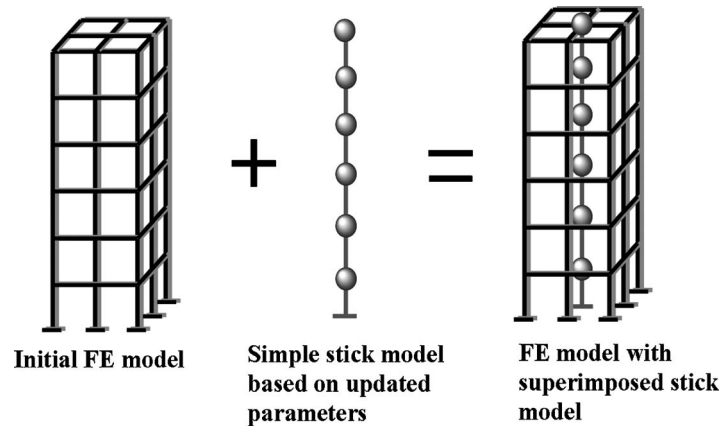
Figure 8. Conceptual example of updating strategy; superimpose a parameter-based stick model into finite element model.

MODEL UPDATING

In general, FE models are established based on the information provided on structural drawings along with idealized assumptions that may not accurately represent the actual structure. As indicated by Table 4, significant discrepancies exist between the modal properties of the initial FE model and those identified from vibration measurements. Model updating is used to achieve an analytical model that yields modal properties that more closely match those identified, and more importantly, predicts the building responses to the given excitation as accurate as possible.

An iterative sensitivity-based method using the identified modal data (frequencies and mode shapes) is utilized to update the initial FE model (Friswell 1995, Link 1999). The modal properties identified using the Parkfield earthquake are used, instead of modal properties identified using ambient vibrations, since they better represent the response of the structure subjected to earthquake ground motions.

The first step in the updating process is to assemble a vector of n physically significant parameters to be updated:

$$P = \{p_1 \ p_2 \ \cdots \ p_n\} \tag{7}$$

in which p_i is the ith parameter. The initial FE model appears to underestimate both the mass and the stiffness of the actual building. It underestimates the mass because contributing live load and the superimposed dead load masses are not considered. Stiffness also is underestimated because the contributions of the NSCs are not considered in the model. To include these contributions, a simple "stick" model with mass and stiffness properties directly related to the parameters to be updated (P) is superimposed into the initial finite element model, exemplified in Figure 8. Each story of the stick model is assigned an effective EW, NS, and torsional stiffness resulting in 45 stiffness parameters.

Table 5. Final additional stiffness and mass quantities (based on updated parameters)

Floor	2nd	3rd	4th	5th	6th	7th	8th	9th	Units
EW Stiffness	794.7	700.4	547.2	406.0	337.0	236.6	378.4	555.4	Kip/in
NS Stiffness	1081.2	982.7	813.2	667.9	587.0	673.3	847.5	1055.2	Kip/in
Torsional Stiffness	891.4	799.5	663.6	544.1	479.8	474.1	592.2	762.4	10^6 kip-in/in
Distributed Weight	5.5	6.0	6.5	7.0	8.6	14.0	20.7	28.5	psf
Floor	10th	11th	12th	13th	14th	15th	Roof	MAX	Units
EW Stiffness	603.3	245.7	291.2	597.1	875.0	1507.3	1248.6	2500	Kip/in
NS Stiffness	1196.3	753.8	1359.9	1884.8	2233.0	2421.8	1951.8	2500	Kip/in
Torsional Stiffness	670.9	887.1	1311.4	1615.0	1730.6	1504.7	1198.7	2000	10^6 kip-in/in
Distributed Weight	31.7	29.8	35.1	40.3	43.0	38.7	36.9	50	psf

The mass quantities (i.e., translational masses and mass moment of inertia) assigned to each node are based on a uniformly distributed weight, resulting in 15 mass parameters. The parameters are defined as ratios, ranging from zero to one, such that the properties assigned to the stick model are the corresponding parameters multiplied by the pre-assigned maximum physical quantities.

Determining the maximum values of the additional stiffness and mass quantities assigned to the stick model requires special considerations and engineering judgment. Depending on the type of NSCs, it is reasonable to assume that the additional story stiffness, provided by the NSCs (mainly interior partitions and $1.5''$ brick veneer), is less than the initial story stiffness provided by the seismic frame. This assumption can be revisited based on the results obtained for the parameters during the updating process. In order to roughly quantify the initial story stiffness, a shear building model of Factor's SMF is constructed. Although the story stiffness values extracted from this model may be greater than the story stiffness values of the complete model, they provide an appropriate starting point to assign stiffness values for the stick model. The weaker story stiffness values (EW, NS, and torsional) of the SMF shear building model are taken as the maximum values for the stiffness quantities in the stick model. Although the Factor Building houses several laboratories with heavy equipment, (e.g., walk-in refrigerators) the additional weight (mass) is likely less than the self-weight of the structure, a direct result of the massive concrete deck. The selected maximum stiffness and mass values for the stick model are listed in the last column of Table 5.

The next step in model updating is to define a residual vector containing the error between the analytical and identified modal data. In order to maintain an overdetermined system of equations, the number of parameters (60) should be less than the number of identified results (135; 9 eigenvalues plus 9×14 independent eigenvector elements). To simplify notation, the following definitions are used:

$$\Omega = \{\omega_1^2 \quad \cdots \quad \omega_9^2\}^{\mathrm{T}} \quad \Phi = \{\phi_1^{\mathrm{T}} \quad \cdots \quad \phi_9^{\mathrm{T}}\}^{\mathrm{T}}$$

$$\bar{\Omega} = \{\bar{\omega}_1^2 \quad \cdots \quad \bar{\omega}_9^2\}^{\mathrm{T}} \quad \bar{\Phi} = \{\bar{\phi}_1^{\mathrm{T}} \quad \cdots \quad \bar{\phi}_9^{\mathrm{T}}\}^{\mathrm{T}} \tag{8}$$

where $\bar{\omega}^2$ and $\bar{\phi}$ are the identified eigenproperties and ω^2 and ϕ are the eigenproperties obtained from the analytical model (the stick model superimposed into the initial FE model). As a result, the vector of analytical eigenproperties is a nonlinear function of the parameter vector P. For the eigenvalues, the residual is defined as the relative difference between the identified and analytically obtained eigenvalues. The relative difference is taken to obtain a similar weighting factor for both the low and high frequencies. For the eigenvectors, each mode shape is first normalized by the roof value (to ensure the comparison of the same ratios) and the residuals are taken as the difference between the identified and analytically obtained mode shapes. The residual vector is defined as

$$\varepsilon = \left\{ \begin{array}{c} (\bar{\Omega} - \Omega) \,.\, /\bar{\Omega} \\ \bar{\Phi} - \Phi \end{array} \right\} \tag{9}$$

where the period before the backslash denotes element-wise division. It is the goal of model updating to determine the set of parameters P that minimizes this error residual. Equation 10 formulates this objective as a constrained nonlinear least-squares minimization problem:

$$\min_{P} \|\varepsilon\|_2^2 \text{ such that } 0 \leq p_i \leq 1 \tag{10}$$

One way to solve Equation 10 is to expand the vector of analytical eigenproperties into a Taylor series that is truncated to include only the linear term (Link 1999):

$$\varepsilon = \left\{ \begin{array}{c} (\bar{\Omega} - \Omega_a) \,.\, /\bar{\Omega} \\ \bar{\Phi} - \Phi_a \end{array} \right\} - \left[\begin{array}{c} \dfrac{\partial \Omega}{\partial P} \,.\, /\bar{\Omega} \\[2mm] \dfrac{\partial \Phi}{\partial P} \end{array} \right]_{P=P_a} \Delta P \tag{11}$$

where Ω_a and Φ_a represent the respective eigenvalues and eigenvectors at the current linearization point (a) and $\Delta P = P - P_a$ is the perturbation vector of parameters. Equation 11 can be expressed in the more compact form as

$$\varepsilon = r_a - S\Delta P \tag{12}$$

where S is the sensitivity matrix defined as

$$S = \begin{bmatrix} \dfrac{\partial \Omega}{\partial P} \ ./\bar{\Omega} \\[2em] \dfrac{\partial \Phi}{\partial P} \end{bmatrix}_{P=P_a} \tag{13}$$

and r_a is the residual at the linearization point a. Consequently, the constrained nonlinear minimization problem becomes a constrained linear minimization problem. Assuming that the initial guess is reasonably close to actual values, Equation 12 can be solved iteratively. The sensitivity matrix in Equation 13 is numerically evaluated for a given iteration using the forward difference method. However, it is often ill-conditioned because various parameters may have a similar influence on the error residuals. This ill-conditioning may yield a solution to Equation 10 that contains large changes in some parameters and small changes in others, which is often not physically sound. To address this issue, an additional parameter constraint is applied based on correlation coefficients between all of the parameter sensitivities, computed as

$$R_{i,j} = \frac{C_{i,j}}{\sqrt{C_{i,i}C_{j,j}}} \tag{14}$$

where C is the covariance of the sensitivity matrix. If, for any two parameters i and j, the corresponding correlation coefficient approaches one, then the two parameters should have similar values, whereas two parameters i and j with a coefficient near zero should not. Negative coefficients are avoided by inverting the result, i.e., assigning values as a function of $1-p_i$. For example, the correlation between a given mass and stiffness parameter is negative because increasing mass has the same effect on the modal properties as the decreasing stiffness. Hence, for a given story, the three stiffness values (EW, NS, and torsional) and the three corresponding mass values (two translational masses and mass moment of inertia) are functions of their corresponding parameters (e.g., the lth, mth, nth, and qth) as

$$k_{EW} = p_l \times 2500 \text{ k/in} \quad k_{NS} = p_m \times 2500 \text{ k/in} \quad k_{Tor} = p_n \times 1.50\text{E}^{09} \text{ k-in/in} \tag{15}$$

$$m = (1 - p_q) \times 50 \text{ psf} \times SF/g \quad I_m = m \times \rho^2$$

where, for the given floor, SF is the area in square feet, ρ is the radius of gyration, and g is the acceleration of gravity. As mentioned earlier, the value of each parameter ranges from zero to one, so the correlation constraint between the ith and jth parameters is simply

$$|p_i - p_j| \leq 1 - R_{i,j} \tag{16}$$

Another important step in the updating process is to assign a weighting matrix (W) to represent the relative confidence in the identified modal properties. In this updating approach, the solution is highly affected by the choice of W (Link 1999). It is apparent

from Figure 4 that the fundamental mode in each direction was excited much more than the higher modes. This is no surprise since the structural response to ground motions is often dominated by the fundamental modes. In addition, significant weight is applied to the eigenvalue residuals to prevent them from being obscured by the many elements in the mode shape residuals. Taking these factors into account, the authors selected a diagonal weighting matrix W is defined as

$$W = I \cdot \{15 \quad 12.5 \quad 12.5 \quad 7.5 \quad 7.5 \quad 7.5 \quad 10 \quad 10 \quad 10 \quad |1 \quad \cdots \quad 1\} \qquad (17)$$

where I is a 135×135 identity matrix and the partition line separates the nine eigenvalue weighting factors from the eigenvector weighting factors. Finally, the minimization problem is expressed as

$$\underset{\Delta P}{\text{Min}} \|WS\Delta P - Wr_a\|_2^2 \text{ such that } 0 \le p_i^k \le 1 \text{ and } |p_i^k - p_j^k| \le 1 - R_{i,j} \qquad (18)$$

where at the kth iteration, $P^k = P^{k-1} + \Delta P$. An implicit function within the MATLAB optimization toolbox is used to solve the minimization problem. The additional stiffness and mass quantities, based on updated parameters and Equation 15 of the stick model, are shown in Table 5 and the modal properties of the updated model are displayed in Table 4. The correlation between the analytical and identified modal properties is drastically improved as a result of model updating.

From inspection of Table 5, it is observed that the additional stiffness provided by the NSCs is greater in the north-south direction than in the east-west direction. This is most likely due to the fact that more brick veneer walls are oriented to contribute in the NS direction. The effect of the additional brick veneer on the upper levels on the west face, Figure 1, is also noted as the upper floors tend to have more additional stiffness than the lower floors.

The predicted response of the updated model to the Parkfield earthquake is compared to the responses derived from measured vibration data to verify the updated model. As means of quantifying the improvement in response prediction as a result of model updating, the relative L_2 norm of the response error (E) is calculated as

$$E = \|a_m(t) - a_p(t)\|_2 / \|a_m(t)\|_2 \qquad (19)$$

where $a_m(t)$ and $a_p(t)$ are the measured and predicted story accelerations, respectively. Figure 9 displays the predicted and measured roof accelerations along with the E for the initial (E_i) and updated (E_u) models. Over the height of the building, the response error tends to decrease with the higher floors. It is noted that the translational responses are improved significantly and are predicted quite well. Although more discrepancy exists for the torsional response, the magnitude of the peak torsional responses are relatively low compared to the peak values for translation. Discrepancies with respect to the amplitude of the response may be the result of inaccurate damping as the identified damping ratios represent classical damping which might not be the actual case. It is also probable that the damping ratios may be time variant; however, varying the damping ratios (within reasonable bounds; ±2%) proved to have little effect on the response error.
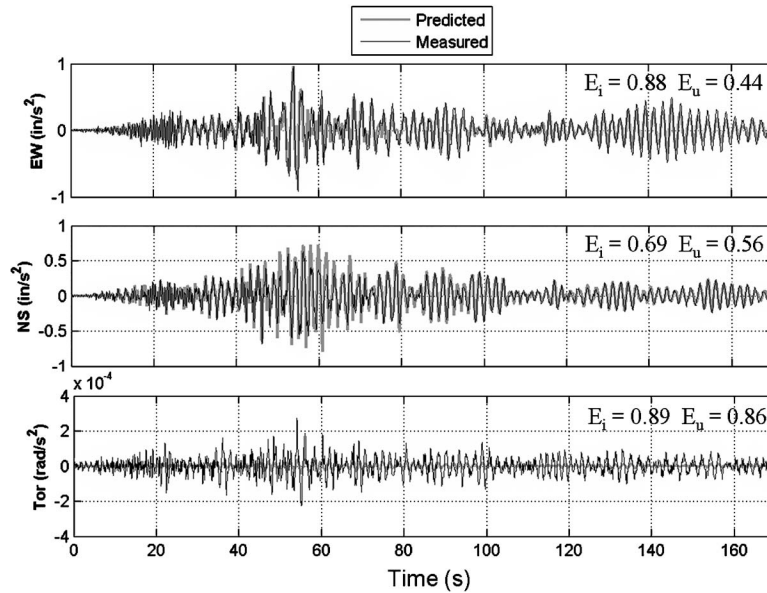
Figure 9. Comparison of predicted and measured roof accelerations for Parkfield earthquake. The L_2 norm of the error between predicted and measured response (E_i for the initial model and E_u for the updated model) is used to quantify the improvement due to model updating.

LARGE-AMPLITUDE RESPONSE PREDICTION

To investigate the response of the Factor Building to larger-amplitude vibrations, recorded ground motions from the 1994 Northridge earthquake from a nearby accelerometer (UCLA Grounds, No. 24688) are obtained and displayed in Figure 10. Since the model is now excited by large-amplitude vibrations, a re-evaluation of previous modeling assumptions is necessary. For example, the no-slip assumption associated with fully elastic composite action may not be reasonable for a structure that experiences significant concrete cracking and possibly inelastic responses. Thus a lower-bound moment of inertia, which considers the horizontal shear force transferred by the shear connectors only, is used based on LRFD (1997) provisions. The values (1.2 to 1.5) of the new modification factors applied to the steel sections to model the composite action are significantly lower than the previous values used to model elastic response. In addition, the partially restrained connections will most likely be loaded beyond their moment capacity; therefore, moment releases are applied at all partially restrained connections (gravity connections). In addition, the contribution of the NSCs should be reduced or possibly ignored. The additional updated mass, however, is not reduced. It is believed that most of the additional mass is due to superimposed dead load, so a mass reduction to account for the sliding of unattached objects in the stronger shaking is not significant.
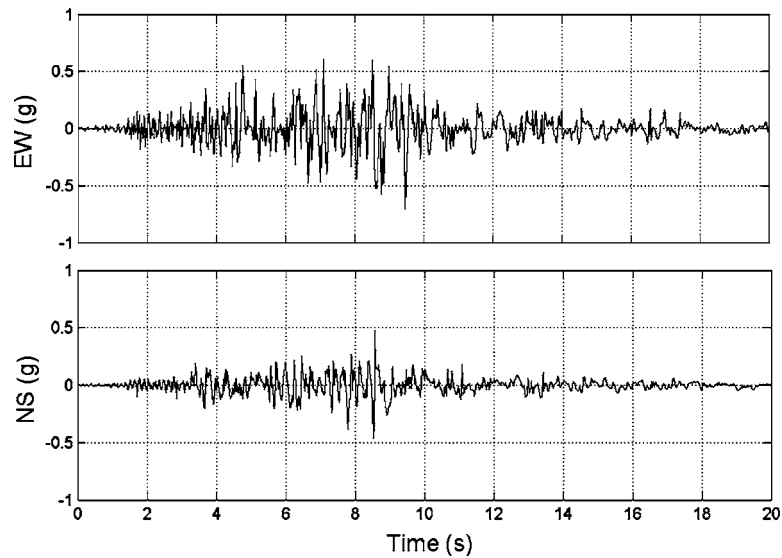
Figure 10. EW and NS ground acceleration components of 1994 Northridge, California, earthquake recorded at UCLA grounds, CSMIP station no. 24688. Station maintained by Strong Motion Instrumentation Program of the California Geological Survey. Data downloaded from the CISN Engineering Strong-Motion Data Center web site.

A linear elastic dynamic analysis is performed under the provisions set forth in *FEMA-356* (ASCE 2000), which is commonly used to evaluate and rehabilitate existing buildings for a prescribed performance level. Obtaining the demand-to-capacity ratios (DCRs) of the SMF members is the primary goal of this analysis. At locations where the DCRs are greater than one, inelastic response is expected and compared with *m*-values published in *FEMA-356* tables to assess if the DCRs are within an acceptable range for a given performance level. According to *FEMA-356*, a linear dynamic procedure (LDP) is applicable if all component DCRs=2.0, or if some DCRs exceed 2.0, but there are no structural irregularities as defined in *FEMA-356*. The Factor Building does not contain an irregularity. In accordance with *FEMA-356*, the capacity of beam-column elements is determined using equations given in AISC (1997) seismic provisions for shear and axial-flexural interaction, except that ϕ shall be taken as unity and nominal yield strengths are replaced with expected yield strengths taken from *FEMA-356* Tables 5-2 and 5-3. According to *FEMA-356*, the DCRs of the beam-column elements are based on their classification as either deformation-controlled ($P_u/P_n \leq 0.5$) or force-controlled ($P_u/P_n > 0.5$), as shown in Equation 20:
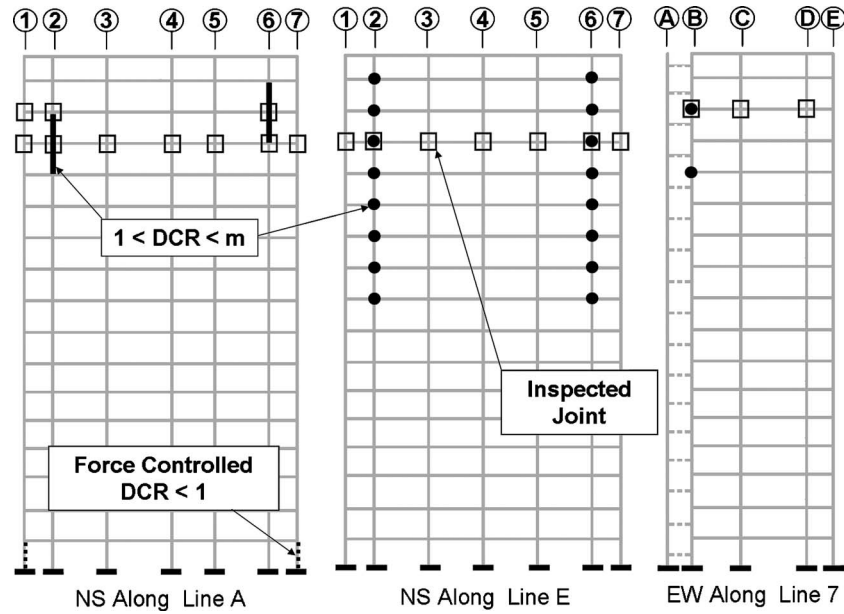
Figure 11. DCR distribution along with locations of joints selected for inspection during the post-earthquake damage evaluation due to the 1994 Northridge event.

$$\text{For } \frac{P_u}{P_n} < 0.2 \qquad \text{DCR} = \frac{P_u}{2P_n} + \frac{M_{ux}}{m_x M_{nx}} + \frac{M_{uy}}{m_y M_{ny}}$$

$$\text{For } 0.2 \leq \frac{P_u}{P_n} \leq 0.5 \quad \text{DCR} = \frac{P_u}{P_n} + \frac{8}{9}\left(\frac{M_{ux}}{m_x M_{nx}} + \frac{M_{uy}}{m_y M_{ny}} \right) \tag{20}$$

$$\text{For } \frac{P_u}{P_n} > 0.5 \qquad \text{DCR} = \frac{P_u}{P_n} + \frac{M_{ux}}{m_x M_{nx}} + \frac{M_{uy}}{m_y M_{ny}}$$

where P_u and P_n are the axial demands and capacities, respectively, M_u and M_n are the flexural demands and capacities ($x=$EW axis, $y=$NS axis), and m values are selected from *FEMA-356* tables. In addition to checking the acceptance of beam-column members, the DCRs corresponding to beam-column joints or panel zones are defined as

$$DCR = \frac{V_u}{m V_n} \tag{21}$$

where V_u and V_n are the panel zone shear demand and capacities, respectively. The results of the LDP are graphically displayed in Figure 11.

An assessment of the building components indicates that several DCRs are greater than one for the Northridge earthquake indicating inelastic responses. However, no

DCRs exceed the *m* values associated with Immediate Occupancy (IO) performance level. Therefore, in agreement with the damage evaluation report, no structural damage is expected. Also, the SMF joints selected for inspection are located among the areas of inelastic response as indicated by the LDP, further validating the analytical results.

It should be noted that, although a LDP approximates deformations reasonably well, a redistribution of loading that occurs as plastic deformations develop is a major drawback associated with LDPs. A nonlinear dynamic analysis would be more accurate; however, given the results reported, is not warranted.

CONCLUSIONS

A successful implementation of the N4SID algorithm identifies modal properties of the first nine modes of a 15-story steel moment-frame building located on the UCLA campus for both low-amplitude earthquake vibrations and ambient vibrations. Confidence in the identification of higher modes is limited by the excitation's low frequency content. The modal frequencies identified from ambient vibrations represent a stiffer structure than those identified from the low-amplitude earthquake excitation. This is believed to be the result of larger contributions to stiffness from nonstructural components for the lower-amplitude events.

An initial FE model is created and updated using a modal-sensitivity-based method with parameters representing the additional mass and stiffness of the building that are not readily modeled. The frequencies and mode shapes of the updated model compare well with those identified from the Parkfield earthquake. In addition, the predicted acceleration response of the updated model compares quite well with the measured data.

It should be noted that the final updated parameters (P) depend on the user-defined weighting matrix and constraints and therefore, are not unique despite the dense sensor array in the Factor Building. Investigation into the minimum number of sensors needed to achieve reasonable identification and updating results would be an interesting study.

The updated model is adjusted to predict the Factor Building's response to a scenario earthquake taken as a record of the 1994 Northridge earthquake. Modest inelastic responses are predicted; however, no significant structural damage is predicted, which is consistent with the findings in the 1994 post-earthquake damage evaluation report. The documentation provided on the building, and the creation and validation of a baseline, linear elastic FE model that can be used for future studies, are presented.

ACKNOWLEDGMENTS

REFERENCES

Alvin, K. F., and Park, K. C., 1994. Second-order structural identification procedure via state-space-based system identification, *AIAA J.* **32** (2), 397–406.

American Society of Civil Engineers (ASCE), 2000. *Prestandard and Commentary for the Seismic Rehabilitation of Buildings*, prepared for the SAC Joint Venture, published by the Federal Emergency Management Agency, *FEMA-356*, Washington, D.C.

Bodeux, J. B., and Golinval, J. C., 2001, Application of ARMAV models to the identification and damage detection of mechanical and civil engineering structures, *Smart Mat. Str.* **10**, 479–489.

Bruneau, M., Uang, C., and Whittaker, A., 1998. *Ductile Design of Steel Structure*, McGraw Hill, Boston, MA.

Englekirk and Sabol Consulting Engineers, Inc., 1994. *Earthquake Damage Evaluation for the Louis Factor Building, UCLA CHS Complex Los Angeles, CA*, Job No. 94-G181.

Friswell, M. J., and Mottershead, J. E., 1995. *Finite Element Model Updating in Structural Dynamics*, Kluwer Academic Publishers, Dordrecht, Netherlands.

International Conference of Building Officials (ICBO), 1973. *Uniform Building Code*, Whittier, CA.

Kohler, M., Davis, P., and Safak, E., 2005. Earthquake and ambient vibration monitoring of the steel-frame UCLA Factor Building, *Earthquake Spectra* **21** (3), 715–736.

Leger, P., Paultre, P., and Nuggihalli, R., 1991. Elastic analysis of frames considering panel zones deformations, *Computers & Structures* **39**, 689–697.

Link, M., 1999. Updating of Analytical Models—Basic Procedures and Extensions, *Modal Analysis and Testing*, NATO Science Series, Kluwer Academic Publ.

Ljung, L., 1999. *System Identification—Theory for the User*, Prentice Hall, NJ.

MATLAB, 2004. *The Language of Technical Computing*, Version 7.0, Mathworks.

Safak, E., 1991. Identification of linear structures using discrete-time filters, *J. Struct. Eng.* **117**, 3064–3085.

Skolnik, D., 2005. Identification, Model Updating, and Response Prediction of the Louis Factor Building, master's thesis, University of California, Los Angeles.

Stewart, J. P., Seed, R. B., and Fenves, G. L., 1999. Seismic soil-structure interaction in buildings. II: Empirical findings, *J. Geotech. Geoenviron. Eng.* **125** (1), 38–48.

U.S. Geological Survey (USGS), 2004. *Earthquake Hazards Program.* http://quake.wr.usgs.gov

Van Overschee, P., and De Moor, B., 1994. N4SID: Subspace algorithms for the identification of combined deterministic-stochastic systems, *Automatica* **30** (1), 75–93.